Electronic Supplementary Information

Oxygen reduction reaction on neighboring Fe-N_4 and quaternary-N sites of pyrolized Fe/N/C catalyst

Adhitya G. Saputro[1] and Hideaki Kasai*[1,2,3]

[1]Department of Applied Physics, Graduate School of Engineering, Osaka University, Suita, Osaka 565-0871, Japan.
[2]Center for Atomic and Molecular Technologies, Osaka University, Suita, Osaka 565-0871, Japan.
[3]Center for Continuing Professional Development, Osaka University, Suita, Osaka 565-0871, Japan.

1 Formation of a z_1-like edge from a perfect z_{211} edge in the presence of an Fe-N_4 site

In this section, we discuss about the formation energy of Fe-N_4 active site located close to the zigzag edge of clean and N-doped z_{211}-GNR systems (Fe-N_4-edge-z_{211}-GNR). Schematic for some of possible active sites formations are shown in Figs. S1 (a)-(d). Positions of N-doped site at zigzag edge in Figs. S1 (c) and (d) are obtained by comparing the relative energies for each of their respective doping configurations (quaternary-N and pyridinium-N, respectively). The supercell for perfect z_{211}-GNR system is shown in Fig. S1 (a). We consider vacuum regions of 15 Å on both of y and z directions. The formation energy ΔE_{form} of Fe-N_4-edge-z_{211}-GNR is evaluated by the following equation:

$$\Delta E_{\text{form}} = E_{\text{defect}} + n_C\mu_C + n_H\mu_H - (n_N\mu_N + \mu_{Fe} + E_{z_{211}}), \quad (1)$$

where ΔE_{defect} and $E_{z_{211}}$ are the total energies of defective z_{211}-GNR and perfect z_{211}-GNR, respectively. n_i (i = C, N, H) is a positive (negative) integer indicating the number of atomic species added to (removed from) the perfect z_{211}-GNR. μ_C is the chemical potential of carbon atom defined as energy per carbon atom in a perfect pristine graphene. μ_H is the chemical potential of hydrogen atom defined as half of total energy of isolated hydrogen molecule. μ_{Fe} is chemical potential of iron defined as energy per

*email address: kasai@dyn.ap.eng.osaka-u.ac.jp

iron atom in its bcc bulk phase. μ_N is the chemical potential of nitrogen calculated by considering two reservoirs: nitrogen molecule and graphitic carbon nitride (g-C_3N_4), which energy difference is found to be 0.54 eV [1, 2]. The variation in the value of μ_N is considered to take into account different nitrogen precursors in experiments[3].

Results of formation energies calculations are shown in Fig. S2. We find that the ΔE_{form} of Fe-N_4-edge-z_{211}-GNR and N-doped Fe-N_4-edge-z_{211}-GNR systems become exothermic at high μ_N. This indicates that FeN_4-edge sites could be formed under N-rich conditions (i.e. under elevated NH_3 flow). Similar result also has been reported for the formation of TM-N_4 center incorporated in a graphene without the presence of any edges [1]. Trend of relative stability of N-doped site of the Ndoped-Fe-N_4-edge-z_{211}-GNR still follows the same trend as in the N-doped z_{211}-GNR system ($E_{\text{pyridinium-N}} < E_{\text{quaternary-N}}$) [4].

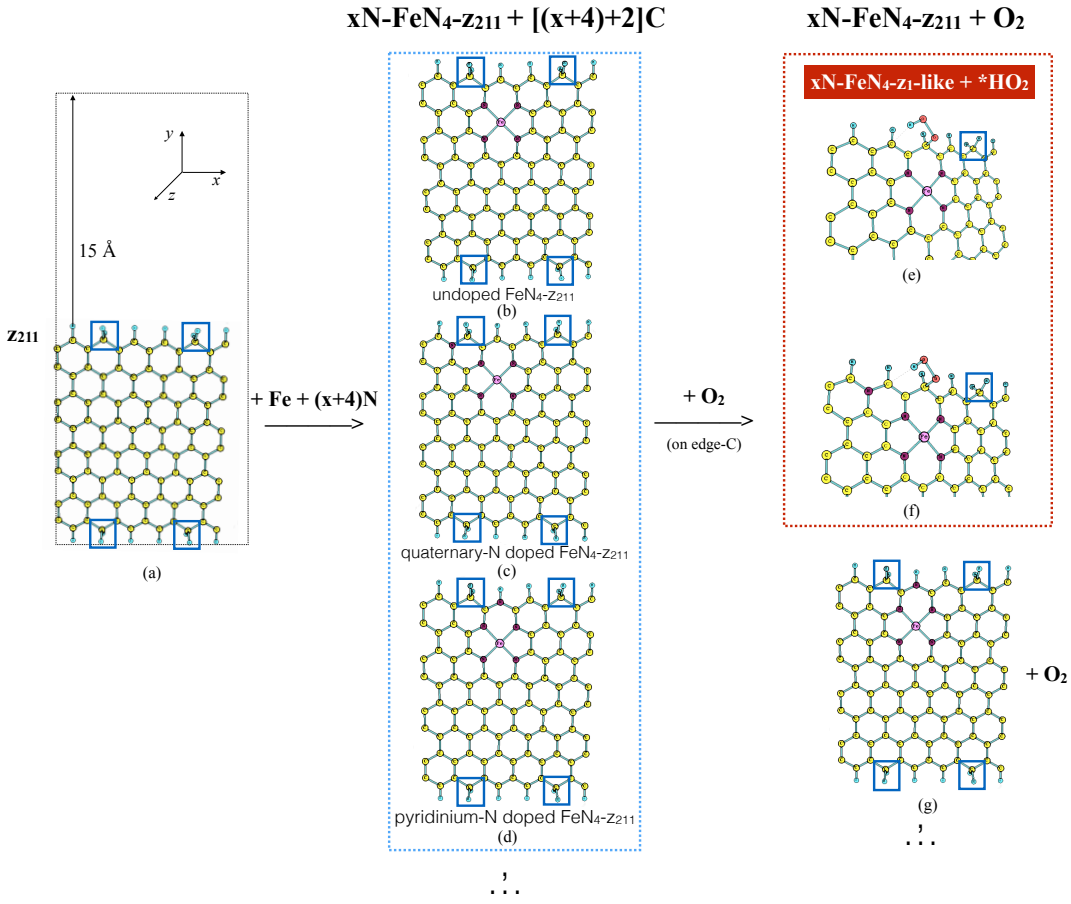

Figure S1: Some possible schemes for the formation of Fe-N_4-edge site at the edge of z_{211} (a)-(d). (e)-(g) show some possible schemes for the formation of Fe-N_4-edge-z_1-like-GNR configurations in the presence of O_2 molecule. Blue squares indicate CH_2 terminated edge-C atoms.

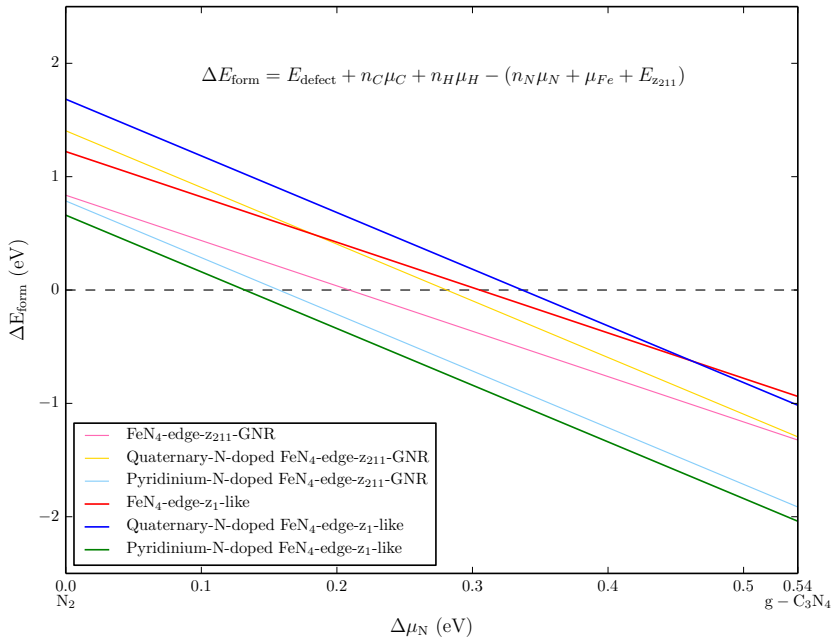

Figure S2: Formation energies of Fe-N_4-edge configurations from a perfect z_{211}-GNR.

Now we check the possibility of the formation of z_1-like edge from a perfect z_{211} edge in the presence of an Fe-N_4-edge site. To do this, we adsorb an O_2 molecule at an edge-C atom next to the Fe-N_4 site. We find that in case of undoped and quaternary-N-doped Fe-N_4-edge-z_{211}-GNR systems, O_2 molecule could be adsorbed on the C atom and spontaneously cleaved the C-H bond of a neighboring CH_2 terminated edge-C atom of z_{211} edge [see Figs. S1 (e) and (f)].

Therefore, we can assume that z_1-like edge configuration could be formed from undoped and quaternary-N doped Fe-N_4-edge-z_{211}-GNR in the presence of an adsorbed O_2 molecule. However, the z_1-like edge configuration could not be formed in the pyridinium-N-doped Fe-N_4-edge-z_{211}-GNR system. This is because pyridinium-N-doped zigzag edge is not active toward O_2 molecule.

We also calculate formation energies of Fe-N_4-edge-z_1-like and N-doped Fe-N_4-edge-z_1-like configurations by removing one hydrogen atom from their corresponding Fe-N_4-edge-z_{211}-GNR configurations (Fig. S2). We find that formations of undoped and quaternary-N-doped Fe-N_4-edge-z_1-like-GNR are relatively less exothermic than that in their corresponding Fe-N_4-edge-z_{211}-GNR configurations. This indicates that these two Fe-N_4-edge-z_1-like configurations are easier to be formed with the help of an O_2 molecule. We also find that the formation of pyridinium-N-doped Fe-N_4-edge-z_1-like configuration is slightly more exothermic than that in pyridinium-N-doped Fe-N_4-edge-z_{211}-GNR configuration. This result indicates that the pyridinium-N-doped Fe-N_4-edge-z_1-like configuration could be easily formed without the help of an O_2 molecule.

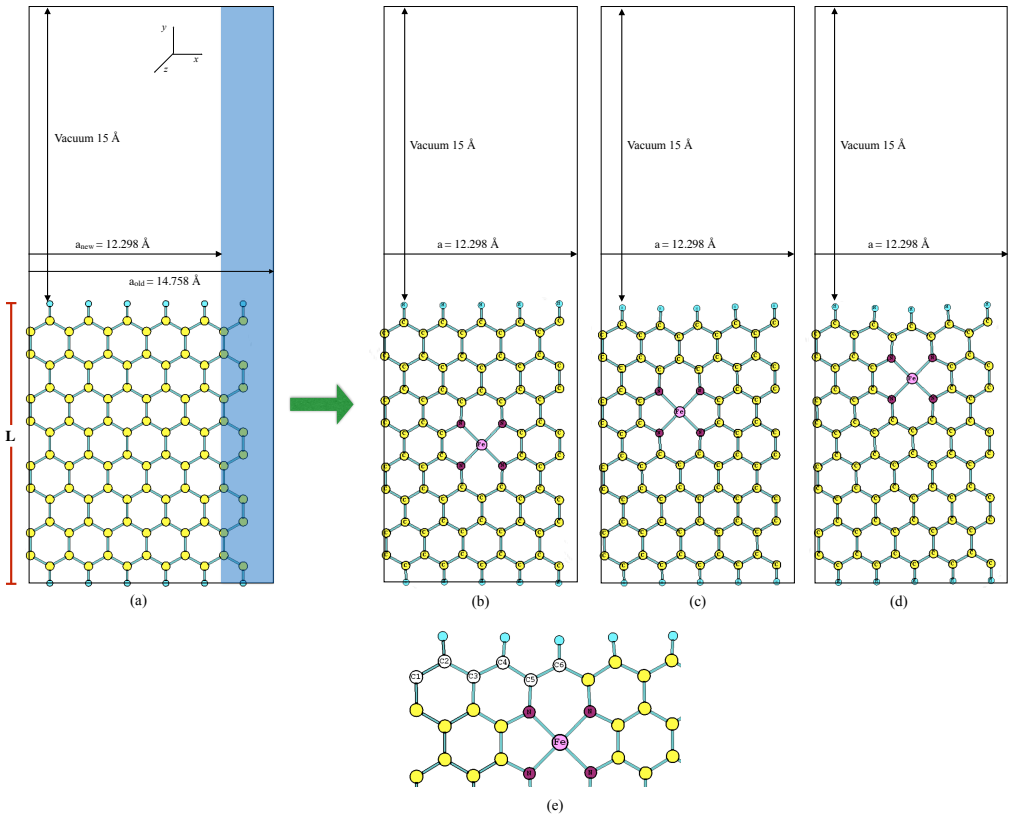

Figure S3: Final supercell models which are used in the study [(b)-(d)] made from the initial super cell model (a). (e) shows indexes of edge-C atoms.

Based on these considerations, we could further simplified our system by the following approximations:

1. Since the z_1-like edge configuration could be recovered during ORR condition (i.e in the presence of O_2 molecule), we could approximate this z_1-like edge by a perfect z_1 edge configuration.

2. Edge states on both of zigzag edges in a ZGNR become nearly decoupled when both of edges are widely separated [5, 6, 7]. Therefore, we can use z_1 edge configuration for both of edges in our model instead of a mix between z_{211} and z_1 edges as in Figs. S1 (e) and (f).

3. Since we are not restricted by the stoichiometry of z_{211}-GNR anymore, we can slightly reduce the lattice parameter in x direction as shown in Fig. S2 (a) to save computational time. The number of zigzag lines across the width of the ribbon is set to eight. This is to maintain the condition in point (2) and to accommodate three distinct configurations of Fe-N_4 site as shown in Figs. S3 (b)-(d). The purpose

of this condition is to compare the relative stability of the Fe-N_4 site in the presence of zigzag edges.

Once the most stable configuration of Fe-N_4 site is found, we substitute edge-C atoms by an N atom[1] and compare the relative stability for each of N-doped configurations.

2 Stability of quaternary-N doped and pyridinium-N doped Fe-N_4-edge-z_1-GNR

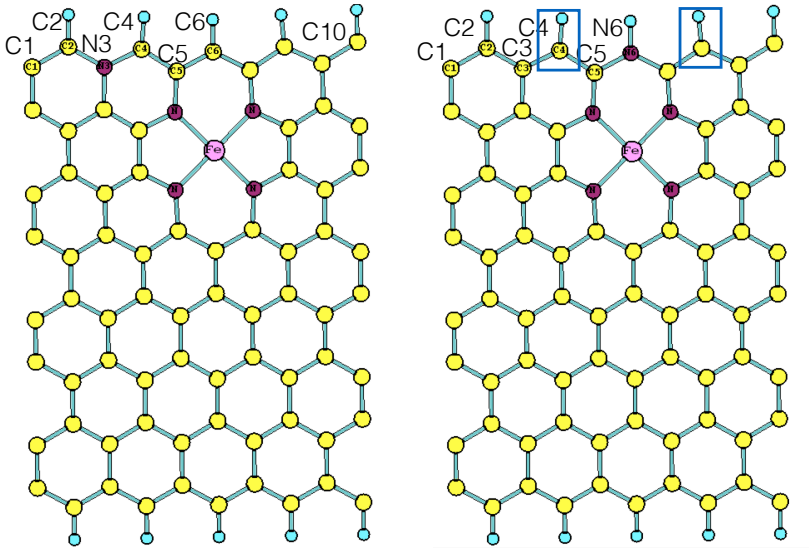

Figure S4: The most stable configuration for quaternary-N-doped Fe-N_4-edge-z_1-GNR (a) and pyridinium-N-doped Fe-N_4-edge-z_1-GNR (b). The number in square brackets represent the relative energy between both configurations.

The most stable configuration for quaternary-N-doped Fe-N_4-edge-z_1-GNR and pyridinium-N-doped Fe-N_4-edge-z_1-GNR are shown in Figs. S4(a) and (b), respectively. The relative stability of N-doped configurations on Fe-N_4-edge-z_1-GNR system still follows the same trend as in the N-doped z_1-GNR system ($E_{\text{pyridinium-N}} < E_{\text{quaternary-N}}$) [8]. Sheng-Feng et al. show that the presence of pyridinium-N-doped at the edge of z_1-GNR stabilizes localized edge-states at the N-doped site and at neighboring CH sites [indicated by blue squares in Fig. S4(b)] by pulling down both of occupied and unoccupied localized anti-bonding edge-states into far bellow the Fermi level. However, the presence of a quaternary-N-doped at the edge of z_1-GNR only pulls down unoccupied localized anti-bonding edge-states slightly below the fermi level [8]. The situation is a little different

[1]The location of N-doped edge-C atoms are shown in Fig. S3 (e)

when an Fe-N_4 site is located close the zigzag edge as in the Fe-N_4-edge-z_1-GNR system. The presence of a pyridinium-N-doped at N6 site[4] could only pull down unoccupied localized anti-bonding edge-states at C2 and C4 sites (indicates by shaded yellow box in Fig. S5) into slightly below the Fermi level [Figs. S5(c) and (f)] as in the quaternary-N-doped case [Figs. S5(b) and (e)]. However, the magnitude of these localized anti-bonding edge-states is significantly reduced, especially at the N6 site. Therefore, the stabilization of the pyridinium-N-doped Fe-N_4-edge-z_1-GNR over the quaternary-N-doped Fe-N_4-edge-z_1-GNR is due to the stabilization and the suppression of its localized anti-bonding edge-states.

Figures S5(j)-(l) show LDOS of Fe atom projected on d-orbitals of undoped Fe-N_4-edge-z_1-GNR, pyridinium-N-doped Fe-N_4-edge-z_1-GNR, and quaternary-N-doped Fe-N_4-edge-z_1-GNR systems, respectively. There are some slight shifts in d_{xz}-orbitals of the spin-down channel indicated by shaded red squares in Figs. S5(j)-(l), while shifts in other d-orbitals are unnoticeable. Due to this similarity, we expect that molecular adsorption strength on top of the Fe atom of these Fe-N_4 sites will not significantly change.

[4]See Figs. S4a and b for the index of edge-C/N atoms of the quaternary-N-doped Fe-N_4-z1-GNR and the pyridinium-N-doped Fe-N_4-z1-GNR, respectively.

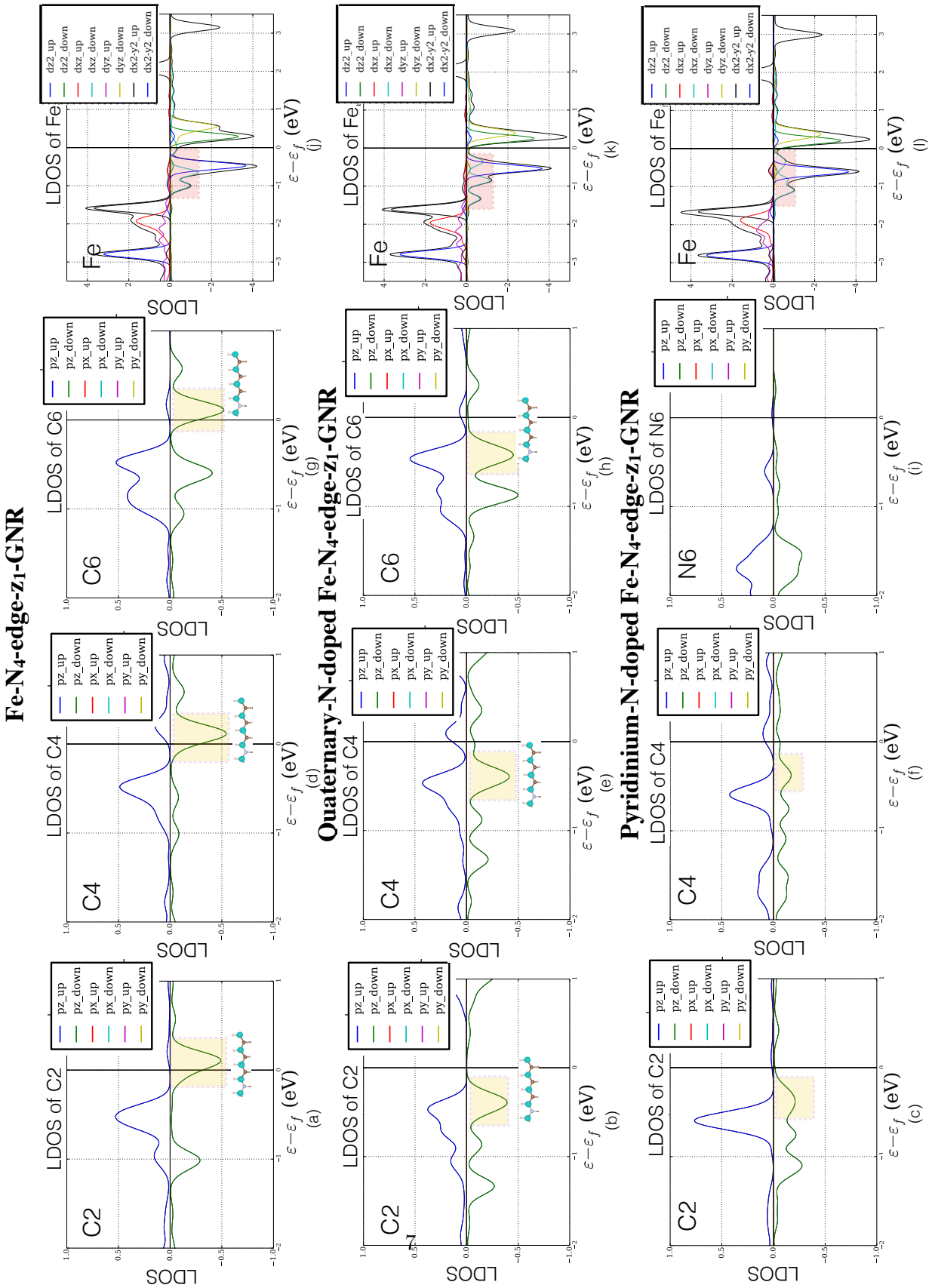

Figure S5: LDOS of C2 (a)-(c), C4 (d)-(f), and C6 (g)-(i) projected on p-orbitals. (j)-(l) show LDOS of Fe atom projected on d-orbitals. Indexes of edge-C/N atoms for the undoped Fe-N_4-z_1-GNR, the quaternary-N-doped Fe-N_4-z_1-GNR, and the pyridinium-N-doped Fe-N_4-z_1-GNR systems are defined in Fig. S3(e), Fig. S4(a) and Fig. S4(b) respectively.

3 Additional figures

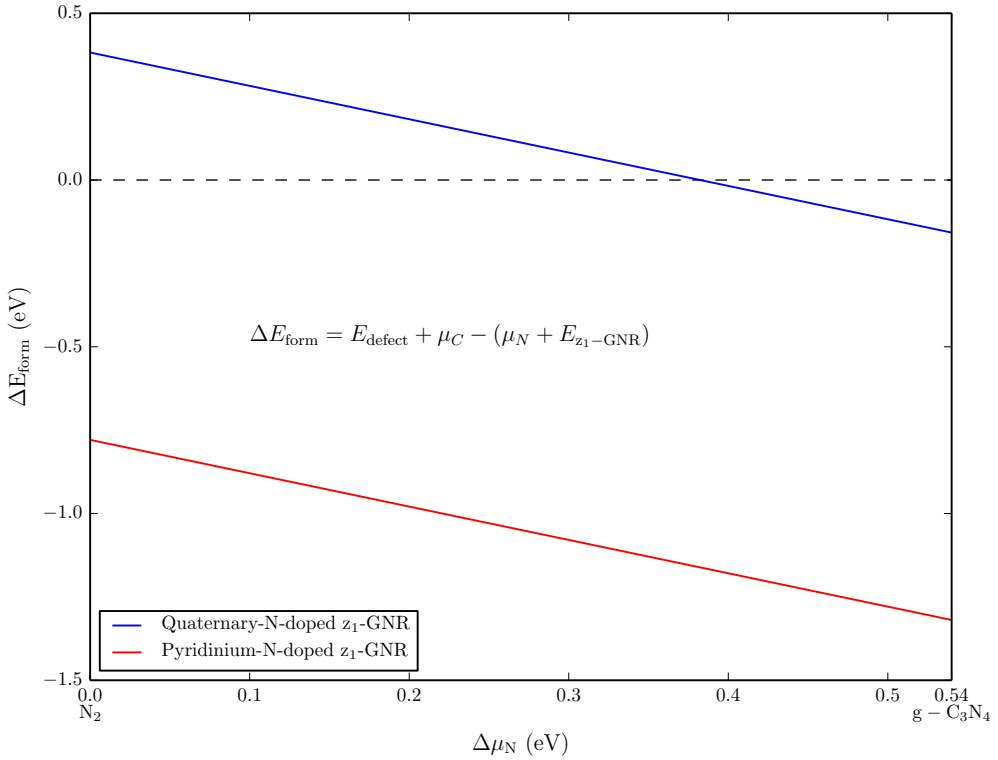

Figure S6: Formation energies of quaternary-N-doped z_1-GNR and pyridinium-N-doped z_1-GNR.

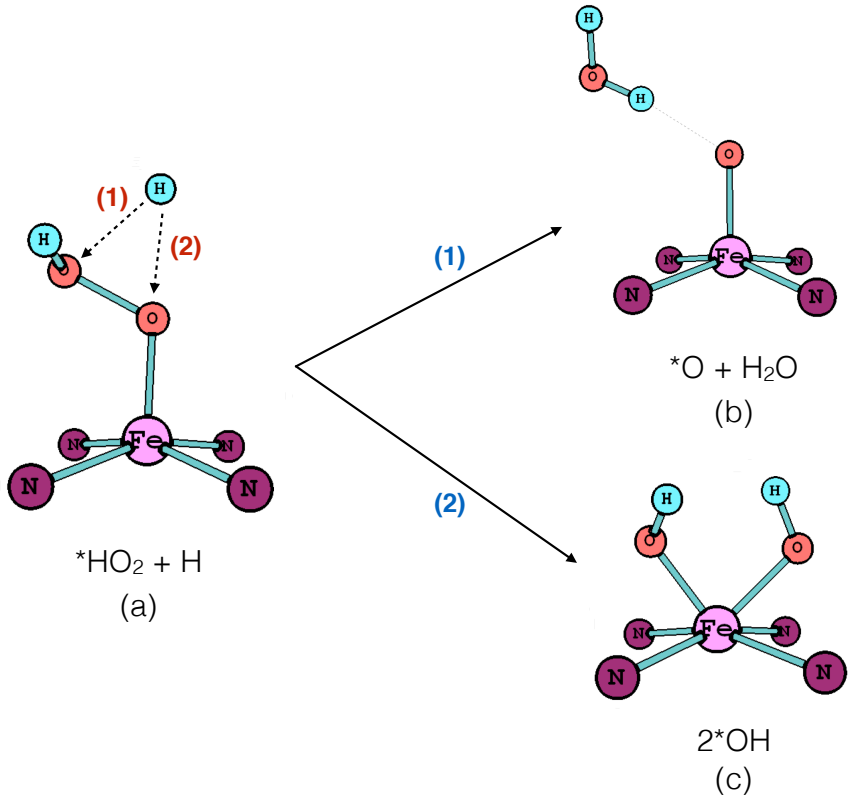

Figure S7: Possibilities for adding an H atom to a pre-adsorbed HO_2 molecule (a) and products of the reaction (b-c).

References

[1] W. Orellana, "Catalytic properties of transition metal-N_4 moieties in graphene for the oxygen reduction reaction: Evidence of spin-dependent mechanisms," *J. Phys. Chem. C*, vol. 117, no. 19, pp. 9812–9818, 2013.

[2] Y. Feng, F. Li, Z. Hu, X. Luo, L. Zhang, X.-F. Zhou, H.-T. Wang, J.-J. Xu, and E. G. Wang, "Tuning the catalytic property of nitrogen-doped graphene for cathode oxygen reduction reaction," *Phys. Rev. B*, vol. 85, p. 155454, Apr 2012.

[3] H. R. Byon, J. Suntivich, and Y. Shao-Horn, "Graphene-based non-noble-metal catalysts for oxygen reduction reaction in acid," *Chem. Mater.*, vol. 23, no. 15, pp. 3421–3428, 2011.

[4] X. Wang, Z. Hou, T. Ikeda, S.-F. Huang, K. Terakura, M. Boero, M. Oshima, M.-a. Kakimoto, and S. Miyata, "Selective nitrogen doping in graphene: Enhanced catalytic activity for the oxygen reduction reaction," *Phys. Rev. B*, vol. 84, p. 245434, Dec 2011.

[5] H. Lee, Y.-W. Son, N. Park, S. Han, and J. Yu, "Magnetic ordering at the edges of graphitic fragments: Magnetic tail interactions between the edge-localized states," *Phys. Rev. B*, vol. 72, p. 174431, Nov 2005.

[6] J. Jung, T. Pereg-Barnea, and A. H. MacDonald, "Theory of interedge superexchange in zigzag edge magnetism," *Phys. Rev. Lett.*, vol. 102, p. 227205, Jun 2009.

[7] J. Kunstmann, C. Özdoğan, A. Quandt, and H. Fehske, "Stability of edge states and edge magnetism in graphene nanoribbons," *Phys. Rev. B*, vol. 83, p. 045414, Jan 2011.

[8] S.-F. Huang, K. Terakura, T. Ozaki, T. Ikeda, M. Boero, M. Oshima, J.-i. Ozaki, and S. Miyata, "First-principles calculation of the electronic properties of graphene clusters doped with nitrogen and boron: Analysis of catalytic activity for the oxygen reduction reaction," *Phys. Rev. B*, vol. 80, p. 235410, Dec 2009.